Optical switching in metal tunnel-insulator n-p^+ silicon devices

S. Moustakas, J.L. Hullett, R.B. Calligaro, A.G. Nassibian and D.N. Payne

Indexing terms: *Metal-insulator-semiconductor devices, Photoelectric devices, Semiconductor switches*

Abstract: This paper considers the mechanism of optical switching and the possible utilisation of the metal tunnel-insulator n-p^+ silicon device in optical communication systems. The pertinent design approaches are described. Under optical excitation, photo holes and electrons generated in the surface depletion region, or within diffusion range, will eventually be separated by the electric field and produce an increment in the forward current. Those hole-electron pairs generated in the junction region, or within diffusion range, produce a photovoltaic increase in the p^+-n junction bias. Switching is induced optically, as it is electrically, by the build up of holes at the insulator-semiconductor interface. This paper employs the 1-dimensional diffusion equation to derive the light-generated minority carrier distributions and diffusion currents in the neutral n and p^+ regions, together with the currents in the surface and p^+-n junction depletion regions. The calculated values of both the drift and diffusion currents compare favourably with those observed experimentally.

1 Introduction

The electrical switching mechanism of the metal-tunnel insulator-n-p^+ silicon structure has recently been described by Simmons, El Badry and Chik.[1-3] Such a device is compatible with i.c. fabrication techniques[1] and hence has potential in commercial i.c. digital circuits. The added ability to switch under optical excitation may lead to further applications in optical communication systems.[4] In this paper we consider the mechanism responsible for optical switching.

Those devices with a lightly doped n-section switch electrically from the high-impedance off state to the low impedance on state when, with increasing forward bias, the depletion region of the n-section reaches through to the p^+-n junction. Up to the point of switching, the normal tendency to form an inversion layer is prevented by holes tunnelling through the thin oxide from the semiconductor to the metal electrode. Switching can also be induced optically and, depending on the design of the structure, the device can be made quite optically sensitive.

The 1-dimensional diffusion equation is employed to derive the light-generated minority carrier distributions and hence diffusion currents in the neutral n and p^+ regions. The drift photocurrents in the surface and p^+n junction depletion regions are also considered. These light-generated current components are shown to be responsible for both a photovoltaic increase in the p^+n junction voltage and a collapsing of the surface depletion region. Depending on the applied external bias, the device will then either remain in its off state or switch to its on state.

Experimental verification of the photocurrent levels and the photovoltaic increase in the p^+n junction voltage was undertaken. For ease of experimentation, an He-Ne red laser was used in the tests.

Possible improvements in the sensitivity of the device as an optical switch are outlined.

Paper T386 S, first received 6th February, and in revised form 4th May 1979

The authors, with the exception of Dr. Payne, are with the Department of Electrical & Electronic Engineering, University of Western Australia, Nedlands, Western Australia, 6009. Dr. Payne is with the Department of Electronics, University of Southampton, Southampton, England S09 5NH

2 Electrical switching mechanism

A schematic diagram of the physical structure of the device is shown in Fig. 1. It comprises a number of layers: an aluminium cathode layer evaporated onto a thin tunnel oxide, followed by an epitaxially grown n-region on a p^+ substrate. Electrical contact is made to the p^+-region by means of a metal anode. Furthermore, a metal gate electrode has been evaporated onto the device adjacent to the cathode. Separation between the two terminals consists of a thick (nontunnelling) oxide.

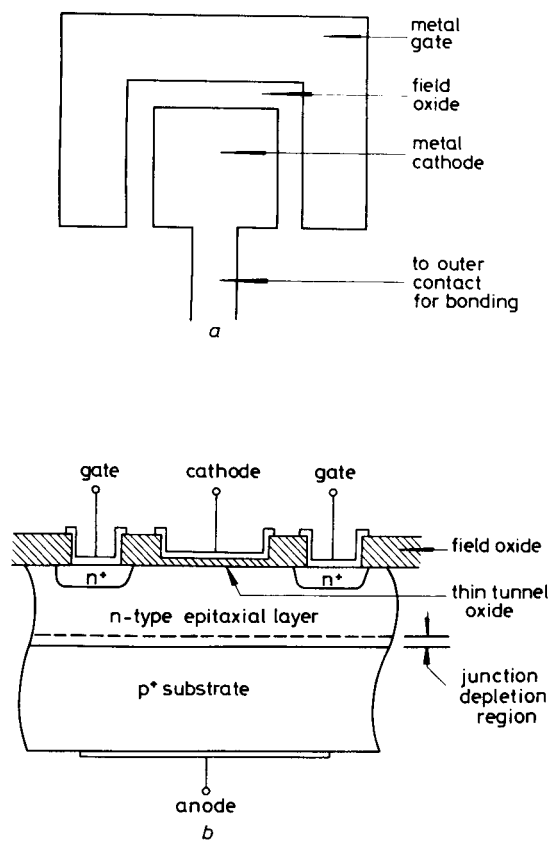

Fig. 1 *Schematic of the physical structure of the device*

a Top view
b Cross-sectional view
(Not to scale)

0308-6968/79/030085 + 09 $01·50/0

The forward I/V characteristic of the silicon structure with the gate electrode floating is shown in Fig. 2*a*. It comprises three parts: a high-impedance low-current off state, a negative-resistance switching state, and a low-impedance high-current on state. Furthermore, as the characteristic resembles that of a thyristor, the device is known as a metal-insulator-semiconductor thyristor or m.i.s.t.

Forward biasing of the m.i.s.t. is effected by operating the cathode negative with respect to the anode (Fig. 2*b*). Under this condition, free electrons are swept away from the surface and a depletion region is established in the n-section under the cathode. Conversely, holes entering or generated within this region are swept away to the oxide-silicon interface where they tunnel through the thin oxide into the metal. Thus, as the bias is increased, the normal tendency to invert the surface is prevented and the surface depletion region continues to grow towards the p^+-n junction. The semiconductor surface is then said to be in deep depletion. The off state current in this mode is limited by generation in the depleted surface region,[1-3] and by recombination in the junction depletion region.

At a sufficiently high forward bias V_s, the surface depletion region punches through to the p^+-n junction space-charge region. Any further increase in the applied bias voltage will effectively lower the potential-barrier height of the p^+-n junction, causing a rush of holes to be injected from the p^+ substrate into the n-type region, where they are swept to the oxide-silicon interface. However, just before punchthrough, the voltage across the oxide is only sufficient to pass the small off-state current. Thus, immediately after punchthrough, the oxide field is insufficient to allow the relatively large injected hole current to tunnel through the thin insulator. Consequently, accumulation of the injected holes takes place at the oxide-silicon interface. Furthermore, electron tunnelling from the metal to the semiconductor condition band has a strong dependence on the free hole density at the semiconductor surface.[5] Those electrons which tunnel through the oxide are then swept by the surface electric field to the p^+-substrate, thus causing a correspondingly larger number of holes to be injected from the p^+-region to the oxide-silicon interface. The free hole density at the semiconductor surface increases further, thereby causing an ever larger electron tunnel current to flow. Hence, a regenerative positive-feedback loop with loop gain greater than unity is established in the device, giving rise to the following two interacting effects:[1]

(*a*) The n-layer begins to move from deep depletion towards inversion, causing the surface potential and, hence, the voltage across the m.i.s.t. to decrease, and the voltage across the load resistor to increase.

(*b*) The field in the oxide begins to increase, allowing a larger current to pass. Thus, a negative resistance region is allowed to develop as the device switches from the off to the on state.

A steady-state operating point is reached when the load resistor current, the p^+-n junction current and the oxide tunnelling current are equal.

Electrical control of the switching process can be realised by either injecting or extracting charged minority carriers through the gate terminal, or by applying a voltage directly to the gate.

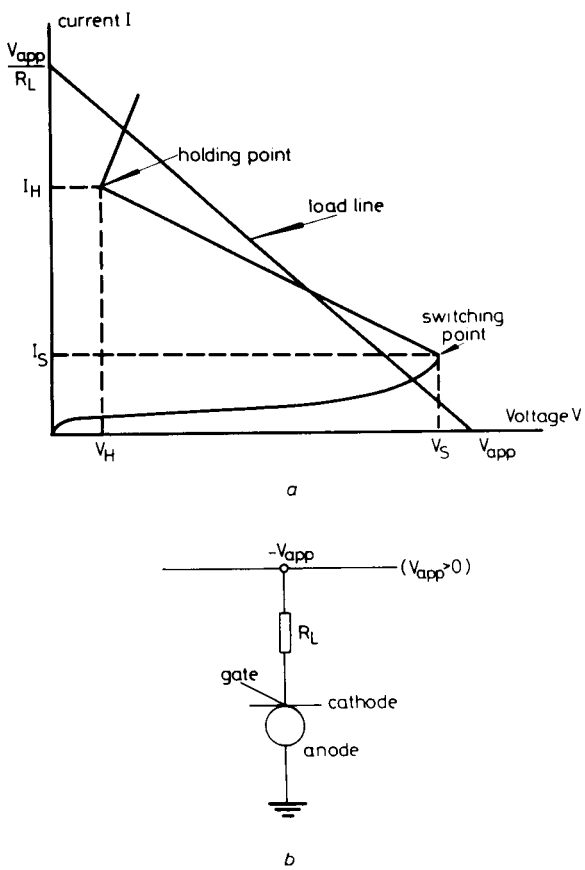

Fig. 2

a I/V characteristic of the device
b Biasing the m.i.s.t.

3 Optically generated currents in the m.i.s.t.

Absorption of light in the m.i.s.t. produces hole-electron pairs at a rate $G(x)$, where[6]

$$G(x) = \eta\Phi_0\alpha e^{-\alpha x} \qquad (1)$$

where η is the effective quantum efficiency, Φ_0 is the total incident photon flux per unit area per second (photons/cm^2 s), and α is the absorption coefficient in cm^{-1}. Both η and α are functions of the optical wavelength and the semiconductor material.[6]

Shown in Fig. 3 is a plot of the rate of optical generation of hole-electron pairs as a function of distance from the cathode of the m.i.s.t. Here, d_{ox}, W_d, W_n and W_j denote the widths of the tunnel oxide, surface-depletion region, neutral n-region and junction depletion region, respectively.

We now consider the regions of the m.i.s.t. where light-generated current components are produced. These are the surface and junction depletion regions where drift currents exist, and the neutral n-region and p^+-substrate where diffusion currents flow.

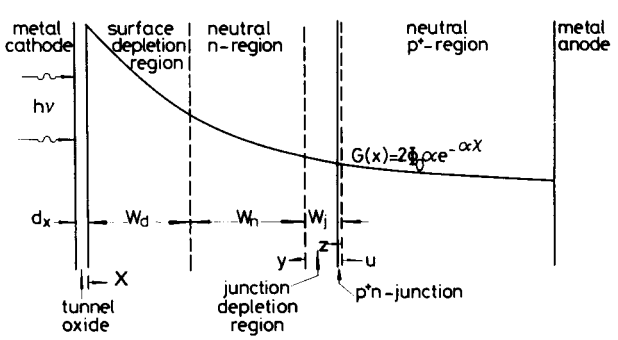

Fig. 3 *Rate of generation of hole-electron pairs due to absorption of light in the m.i.s.t. (not to scale)*

3.1 Surface depletion region

Hole-electron pairs created in the surface depletion region will immediately be separated by the depletion-layer electric field. Electrons are swept to the neutral n-region where they diffuse towards the p^+-n junction space-charge region and recombine with holes injected into the junction depletion region by the small forward bias, while holes are swept to the oxide-silicon interface where they tunnel through the thin SiO_2 layer. If the device is not triggered into the switching mode (see Section 4 for discussion on optical switching), the generated photocurrent contributes directly to the m.i.s.t. off-state current. For a maximum increase in drive current the surface depletion region width is made large relative to the light penetration depth α^{-1}.

The current reaching the oxide-silicon interface, due to optical excitation of hole-electron pairs in the surface depletion region, is given by:[6]

$$I_{dL} = -qA_L \int_0^{W_d} G(x)\,dx$$

$$= -\frac{q\eta\lambda P}{hc}(1 - e^{-\alpha W_d}) \qquad (2)$$

Here, the total incident photo flux Φ_0 was written in terms of the total incident optical power P:

$$\Phi_0 = \frac{P\lambda}{hcA_L}$$

where h is Planck's constant, c and λ are the speed and wavelength of the incident light, respectively, and A_L is the illuminated area. For

$$W_d \gg \frac{1}{\alpha}$$

then

$$I_{dL} \simeq -\frac{q\eta\lambda P}{hc}$$

and a maximum current increase is achieved.

3.2 Junction depletion region

Holes and electrons generated optically in the junction depletion region are swept to the p^+-substrate and epitaxial n-layer, respectively. The resulting current component does not contribute directly to the m.i.s.t. off-state current. However, a photovoltaic increase in the p^+-n junction bias is brought about, and this leads to an increased forward junction current that:

(i) supports the optically generated junction depletion region current

(ii) supports the surface depletion region photocurrent

The photocurrent produced in the junction depletion region is given by

$$I_{jL} = -qA_L \int_0^{W_j} G(z)\,dz \qquad (3)$$

where $G(z)$ has been defined in this region as

$$G(z) = \eta \frac{P\lambda}{hcA_L} \alpha e^{+\alpha(z - W_n - W_d - W_j)} \quad 0 < z < W_j$$

Here, $z = 0$ is taken to be at the edge of the junction depletion region and the p^+-substrate (Fig. 3).

Substituting for $G(z)$ in eqn. 3 and evaluating the integral gives the current produced by optical excitation of hole-electron pairs in the p^+-n junction depletion region as

$$I_{jL} = -\frac{q\eta\lambda P}{hc}\left[e^{-\alpha(W_n + W_d)} - e^{-\alpha(W_n + W_d + W_j)}\right] \qquad (4)$$

3.3 Neutral n-region

Optical generation of hole-electron pairs in the neutral n-regions results in two current components flowing in opposite directions. The components are due to the diffusion of photoholes to either the surface or junction depletion regions. Photoholes reaching the surface depletion region are swept to the oxide-silicon interface where they tunnel through the thin SiO_2 layer. If the device is not triggered into the switching mode, this generated photocurrent contributes directly to the m.i.s.t. off-state current. Photoholes diffusing to the junction depletion region are swept to the p^+-substrate by the electric field present within the junction space-charge region. They then contribute to a photovoltaic increase in the p^+n junction bias.

As linear superposition applies to the junction bias current and the photocurrent,[7] then the two optically generated current components can be determined from the photohole (or minority carrier) gradient on either side of the neutral n-layer. The distribution of photoholes in the neutral n-region is obtained by solving the steady-state 1-dimensional diffusion equation:[6, 7]

$$D_p \frac{\partial^2 P_{nL}(y)}{\partial y^2} - \frac{P_{nL}(y)}{\tau_p} + G(y) = 0$$

or

$$\frac{\partial^2 P_{nL}(y)}{\partial y^2} - \frac{P_{nL}(y)}{L_p^2} = -\frac{\eta\Phi_0\alpha}{D_p} e^{\alpha(y - W_n - W_d)} \qquad (5)$$

where D_p is the hole diffusivity, τ_p is the minority carrier lifetime, L_p is the minority carrier diffusion length, and the rate of optical generation of hole-electron pairs in the neutral n-layer is given by

$$G(y) = \eta\Phi_0\alpha e^{\alpha(y - W_n - W_d)}$$

Here, $y = 0$ is taken to be at the edge of the junction depletion region and the n-type epitaxial layer, as shown in Fig. 3.

The general solution to eqn. 5 is

$$P_{nL}(y) = Ae^{y/L_p} + Be^{-y/L_p} + \chi_p e^{\alpha(y - W_n - W_d)} \qquad (6)$$

where χ_p is

$$\chi_p = \frac{-\eta\Phi_0}{\alpha D_p\left(1 - \frac{1}{\alpha^2 L_p^2}\right)} \qquad (7)$$

The constants A and B can be determined from the following set of boundary conditions:

(a) Because of the polarity of the electric field in the junction depletion region, photoholes that diffuse to the edge of the junction depletion region will run down a potential energy hill to a more stable lower energy level in the p^+-substrate of the m.i.s.t. Thus, a perfect sink exists

for minority carriers, so that

$$P_{nL}(0) = 0 \tag{8}$$

(*b*) Similarly, the edge of the surface deep depletion region at $y = W_n$ is another sink for minority hole carriers, so that

$$P_{nL}(W_n) = 0 \tag{9}$$

Application of these boundary conditions to eqn. 6, and solving for A and B, gives the distribution of photoholes in the neutral n-region as

$$P_{nL}(y) = \left[\frac{\chi_p e^{-\alpha W_d}(e^{-W_n/L_p}e^{-\alpha W_n} - 1)}{2\sinh\frac{W_n}{L_p}}\right]e^{y/L_p} + \left[\frac{\chi_p e^{-\alpha W_d}(1 - e^{W_n/L_p}e^{-\alpha W_n})}{2\sinh\frac{W_n}{L_p}}\right]e^{-y/L_p} + \chi_p e^{\alpha(y - W_n - W_d)} \tag{10}$$

According to the boundary conditions (eqns. 8 and 9) two light-generated current components may be seen to exist – a smaller component I_{pL} flowing across the p^+-n junction, and a larger component I'_{pL} flowing into the surface depletion region. Each is determined by the minority carrier gradient on either side of the neutral n-layer. That is:

(i) At $y = 0$,

$$I_{pL} = -qD_p\left(\frac{dp_{nL}}{dy}\right)_{y=0}A_L = \frac{q\eta\lambda Pe^{-\alpha W_d}\left(e^{-\alpha W_n}\cosh\frac{W_n}{L_p} + \alpha L_p e^{-\alpha W_n}\sinh\frac{W_n}{L_p} - 1\right)}{\alpha hcL_p\left(1 - \frac{1}{\alpha^2 L_p^2}\right)\sinh\frac{W_n}{L_p}} \tag{11}$$

(ii) At $y = W_n$,

$$I'_{pL} = -qD_p\left(\frac{dp_{nL}}{dy}\right)_{y=W_n}A_L = \frac{q\eta\lambda Pe^{-\alpha W_d}\left(e^{-\alpha W_n} - \cosh\frac{W_n}{L_p} + \alpha L_p\sinh\frac{W_n}{L_p}\right)}{\alpha hcL_p\left(1 - \frac{1}{\alpha^2 L_p^2}\right)\sinh\frac{W_n}{L_p}} \tag{12}$$

However, when no surface depletion region exists (zero bias applied to the cathode of the m.i.s.t.), the boundary condition given by eqn. 9 no longer applies. Thus, I_{pL} and I'_{pL} given by eqns. 11 and 12, respectively, are similarly no longer valid. Under this condition of zero bias, photoholes created in the n-type epitaxial layer of the m.i.s.t. will now only diffuse towards the p^+-n junction depletion region. That is, there is no photocurrent flowing away from the junction, and hence

$$I'_{pL}|_{W_d=0} = 0 \tag{13}$$

For the current I_{pL} flowing across the junction depletion region and into the p^+-substrate, the steady-state diffusion equation must be solved subject to the new boundary conditions:

$$P_{nL}(0) = 0 \tag{8}$$

and

$$P_{nL}(W_n) = G(W_n)\tau_p = \eta\alpha\Phi_0\tau_p \tag{14}$$

where $W_d = 0$.

The second boundary condition is valid only if the hole diffusion length L_p is much less than the width of the neutral n-region W_n. Otherwise, holes created at the surface will diffuse to the edge of the junction depletion region where they will immediately be swept to the p^+-substrate. Consequently, the steady-state concentration of photoholes will be less than that suggested by eqn. 14. However, the m.i.s.t. is fabricated on wafers where, typically, the width of the epitaxially grown n-layer (and hence the neutral n-region for $W_d = 0$) is greater than the hole diffusion length. Therefore, the special case of $L_p \gg W_n$ is not treated.

Application of the boundary conditions (eqns. 8 and 14) to eqn. 6, and solving for the constants A and B, gives the distribution of photoholes in the neutral n-region for $W_d = 0$, as

$$p_{nL}(y)|_{W_d=0} = \left[\frac{\eta\alpha\Phi_0\tau_p + \chi_p(e^{-\alpha W_n}e^{-W_n/L_p} - 1)}{2\sinh W_n/L_p}\right]e^{y/L_p} + \left[\frac{-\eta\alpha\Phi_0\tau_p + \chi_p(1 - e^{-\alpha W_n}e^{W_n/L_p})}{2\sinh W_n/L_p}\right]e^{-y/L_p} + \chi_p e^{\alpha(y - W_n)} \tag{15}$$

The resulting light-generated current flowing across the junction into the p^+-substrate is then determined by the minority carrier gradient at the edge of the junction depletion region:

$$I_{pL}|_{W_d=0} = \frac{-q\eta\alpha\lambda PL_p}{hc\sinh W_n/L_p} + \frac{q\eta\lambda P(e^{-\alpha W_n}\cosh W_n/L_p + \alpha L_p e^{-\alpha W_n}\sinh W_n/L_p - 1)}{\alpha hcL_p\left(1 - \frac{1}{\alpha^2 L_p^2}\right)\sinh W_n/L_p} \tag{16}$$

3.4 Neutral p^+-region

A similar situation exists in the p^+-substrate as in the neutral n-section. Optically generated minority carriers (electrons) within diffusion range of the p^+-n junction will eventually be swept by the electric field toward the n-type epitaxial layer. Thus, a further contribution is made to the photovoltaic increase in the junction bias. Photoholes, on the other hand, will diffuse away from the junction and eventually recombine with the minority carrier electrons.

As linear superposition of the junction bias current and the photocurrent applies,[7] the optically generated current can be determined by the minority carrier photoelectron gradient at the edge of the junction depletion region. The distribution of photoelectrons in the p^+-substrate is obtained by solving the steady-state diffusion equation

$$D_n \frac{\partial^2 n_{pL}(u)}{\partial u^2} - \frac{n_{pL}(u)}{\tau_n} + G(u) = 0$$

or

$$\frac{\partial^2 n_{pL}(u)}{\partial u^2} - \frac{n_{pL}(u)}{L_n^2} = \frac{-\eta\Phi_0\alpha}{D_n} e^{-\alpha(u+W_n+W_d+W_j)} \tag{17}$$

where D_n is the electron diffusivity, τ_n is the minority carrier lifetime, L_n is the minority carrier diffusion length, and the rate of optical generation of hole-electron pairs in the neutral p^+-substrate is given by

$$G(u) = \eta\Phi_0\alpha e^{-\alpha(u+W_n+W_d+W_j)}$$

Here, $u = 0$ is taken to be at the edge of the junction depletion region and the p^+-substrate, as shown in Fig. 3.

The general solution to eqn. 17 is

$$n_{pL}(u) = Ae^{u/L_n} + Be^{-u/L_n} + \chi_n e^{-\alpha(u+W_n+W_d+W_j)} \tag{18}$$

where the term χ_n is defined as:

$$\chi_n = \frac{-\eta\Phi_0}{\alpha D_n\left(1 - \frac{1}{\alpha^2 L_n^2}\right)} \tag{19}$$

The constants A and B are determined from the following boundary conditions:

(*a*) Any photoelectrons reaching the junction depletion region will run down a potential energy hill to a more stable lower energy level in the neutral n-layer of the m.i.s.t. Thus a perfect sink exists for minority carriers, so that

$$n_{pL}(0) = 0 \tag{20}$$

(*b*) Photoholes diffuse away from the junction and eventually recombine with the minority carrier electrons, so that

$$n_{pL}(\infty) = 0 \tag{21}$$

Application of these boundary conditions to eqn. 18, and solving for A and B, gives the distribution of photoelectrons in the p^+-substrate as:

$$n_{pL}(u) = \chi_n e^{-\alpha(W_n+W_d+W_j)}\left[e^{-\alpha u} - e^{-u/L_n}\right] \tag{22}$$

The resulting light-generated current flowing across the p^+-n junction is then determined from the photoelectron gradient at the edge of the junction space-charge region:

$$I_{nL} = qD_n\left(\frac{dn_{pL}}{du}\right)_{u=0} A_L$$

$$= \frac{q\eta\lambda P e^{-\alpha(W_n+W_d+W_j)}}{hc\left(1 + \frac{1}{\alpha L_n}\right)} \tag{23}$$

4 Discussion of the optical switching mechanism

We now consider the mechanism responsible for optically switching a given device biased as shown in Fig. 2.

To switch the m.i.s.t. optically, an inversion layer must still be formed at the surface, as is the case for electrical switching. However, the mechanism responsible for inversion is not punchthrough but rather the generation of photoholes within diffusion range of, or in, the surface depletion region. This creates the current components I_{dL} and I'_{pL} that flow towards the oxide-silicon interface. Furthermore, optical generation of hole-electron pairs within diffusion range of, or in, the junction depletion region result in reverse current components I_{pL}, I_{jL} and I_{nL} which give rise to a photovoltaic increase in the p^+-n junction voltage. Consequently, there is an increase in the injection of holes from the p^+-substrate towards the surface depletion region where they are then swept to the oxide-silicon interface by the surface electric field.* However, at the interface, the oxide voltage is sufficient to pass only the small off-state current, and thus accumulation of both the photoholes and injected holes takes place at the surface. As is the case for electrical switching, the build up of holes results in three interacting effects:

(i) The n-layer begins to move from deep depletion towards inversion, causing the surface potential, and hence the voltage across the m.i.s.t., to decrease, and the voltage across the load resistor to increase.

(ii) The oxide field begins to increase, allowing a larger current to pass.

(iii) Electron tunnelling from the metal to the semiconductor conduction band increases because of its strong dependence on the free hole density at the semiconductor surface.

Increased electron tunnelling results in the electrons being swept by the surface field to the p^+-substrate, thus initiating a further increase in the injection of substrate holes to the oxide-silicon interface. If the oxide voltage is charging up at a rate sufficient to accommodate the second hole injection mechanism, the surface free hole density will begin to decrease, causing the device to remain in the off-state. A steady-state operating point is established in the m.i.s.t. when the currents flowing through the load resistor, the p^+-n junction and the tunnel oxide are equal, and there is a sufficient free-hole density at the surface to sustain the increased oxide voltage. Under these conditions, there is an increase in the m.i.s.t. off-state current with a corresponding decrease in the voltage across the device, as depicted in Fig. 4*a*. This has been observed experimentally (Fig. 4*b*).

As the incident optical power is increased there is an approximately linearly related increase in the forward current components I_{dL} and I'_{pL}, and the reverse current components I_{pL}, I_{jL} and I_{nL}. Consequently, the free hole density at the oxide-silicon interface is increased, causing a larger electron tunnel current to flow, which in turn causes an even greater increase in the injection of substrate holes to the semiconductor surface. Although the oxide field is increasing in response to the surface free-hole density, it becomes increasingly more difficult for the oxide field to accommodate the increased flow of holes to the

*Recombination of injected holes will take place in the neutral n-region. However, as this does not affect greatly the overall discussion of the optical switching mechanism, it is assumed for the sake of clarity that recombination is negligible.

surface. When the rate at which these holes reach the oxide-silicon interface becomes greater than the rate at which holes are tunnelling through the thin oxide, enhanced accummulation takes place at the surface. Hence, a regenerative positive-feedback loop with loop gain greater than unity is established and the device moves into a switching transient. In this mode the surface potential continues to decrease, and the oxide voltage and device current to increase, thus allowing the formation of the negative resistance region in the m.i.s.t. output characteristic as shown in Fig. 4. When the surface becomes inverted, the surface potential no longer decreases but remains fixed at twice the potential difference between the semiconductor Fermi level and intrinsic Fermi level. The oxide voltage, however, continues to increase, thus allowing the low impedance on-characteristic to develop. A steady-state operating point is then reached when there is current continuity through the load resistor, the p^+-n junction and the tunnel oxide.

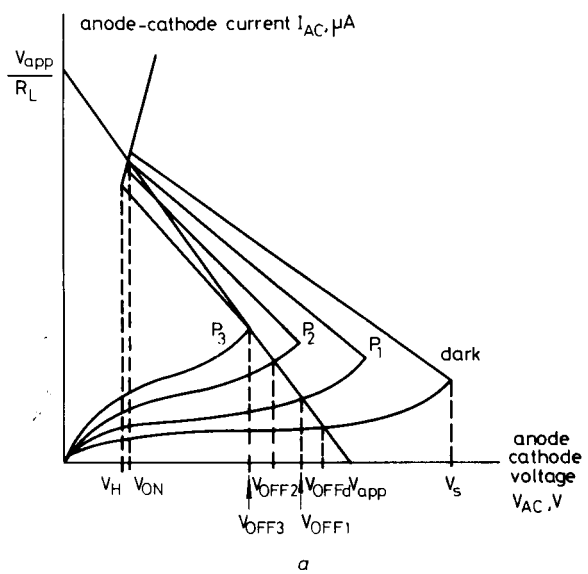

a

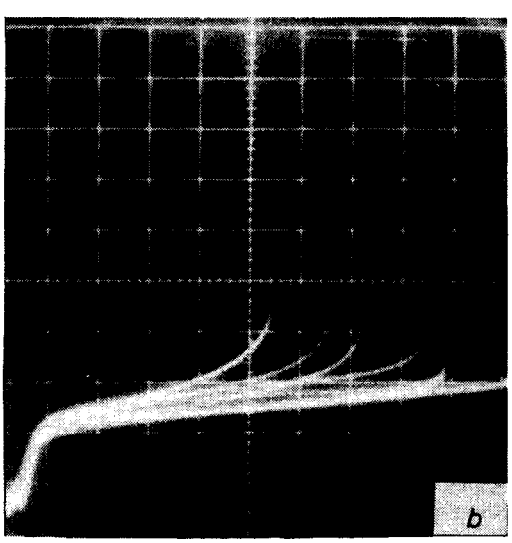

Fig. 4

a *I/V* characteristic of the m.i.s.t. under different intensities of irradiation (not to scale)
b Experimental observations (vertical scale: 1 μA/division, horizontal scale: 1 V/division)

Thus, the processes involved in both electrical and optical switching are basically identical, differing only in the mechanism responsible for initiating inversion of the semiconductor surface. Electrically, and without gate control, inversion is brought about by the surface depletion region punching through to the junction depletion region, whereas, under optical excitation, it is the generation of both photoholes in and around the surface depletion region, and of hole-electron pairs in and around the junction depletion region that is responsible.

The sensitivity of the m.i.s.t. to a constant input optical power can be improved if more holes can be collected at the surface and at a faster rate. These effects can be achieved by implementing the following simple structural changes to the device:

(*a*) increasing the epitaxial layer depth to above the absorption depth of the incident radiation, thus ensuring a near optimum collection efficiency of the generated photoholes

(*b*) decreasing the p^+-n junction area, and hence capacitance, which increases the rate at which the junction voltage charges up to the value fixed by the photovoltaic effect.

However, increasing the epitaxial-layer depth will result in a smaller photovoltaic increase in the junction bias and hence a smaller injection of substrate holes. A compromise situation is therefore created.

5 Optical current continuity in the m.i.s.t. in the off state

Optical switching of the m.i.s.t. takes place when the rate of collection of free holes at the surface is sufficient to initiate a positive regenerative feedback loop with loop gain greater than unity such that inversion of the surface is allowed to occur. However, it was seen in Section 4 that the device may remain in the off state if the rate at which holes are tunnelling through the thin oxide is greater than the rate at which they are being replenished at the surface. A steady-state operating point is then established in the off state when these two rates become equal. We now examine the components of current that bring about this current continuity throughout the device.

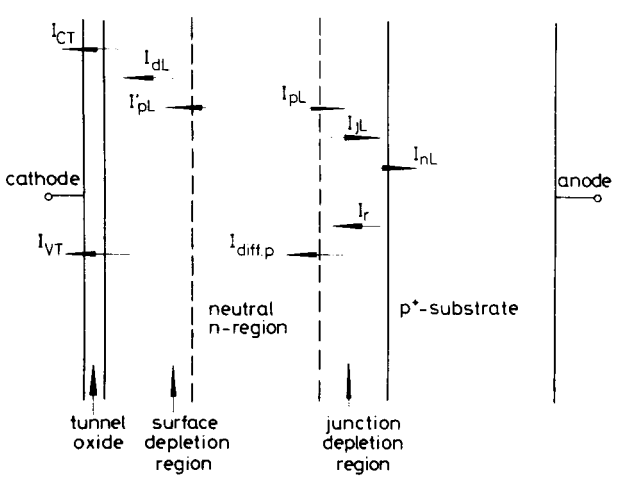

Fig. 5 *Off-state current components in the m.i.s.t. in equilibrium*
All components indicate a positive flow of holes

Shown in Fig. 5. are the off-state current components flowing in the m.i.s.t. when in equilibrium. Here, I_{dL}, I'_{pL}, I_{pL}, I_{jL} and I_{nL} are the optical current components described in Section 3, I_r is the junction recombination current, $I_{diff\,p}$ is the junction hole diffusion current, while I_{CT} and I_{VT} denote the electron and hole tunnelling currents, respectively. All the current components shown indicate a positive flow of holes, although I_{CT} and I_{nL} are due to the flow of electrons. Furthermore, as the p^+-substrate is more highly doped than the n-type epitaxial layer, the junction electron diffusion current $I_{diff\,n}$ has been neglected.[8]

With the device in the dark, the junction voltage is of the order of 0·1 V,[2-4] and thus the junction recombination current dominates the junction hole diffusion current.[8] The source of electrons that feed this recombination current are derived from both electron tunnelling (I_{CT}) from the metal to the semiconductor conduction band and from the thermal generation of electron-hole pairs in the epitaxial layer (I_{VT}). For large junction area devices, it is the electron tunnelling mechanism that dominates. The total current through the device may then be written as:

$$I_{AC_d} = I_r = I_{CT}$$

With the m.i.s.t. excited optically, we may distinguish between two cases. These are when:

(i) the junction hole diffusion current is much less than either the junction recombination current or the light-generation current components I_{dL} and I'_{pL}. This will occur for junction voltages of approximately less than 0·3 V. Under these circumstances there will be no injection of holes from the p^+-substrate to the oxide-silicon interface whereby the surface free hole density will consist solely of photoholes. The corresponding photoelectrons that are swept out of the surface depletion region help feed the junction recombination current, which must also overcome the optical current components I_{pL}, I_{jL} and I_{nL}. The device current is therefore

$$\begin{aligned} I_{AC_L} &= I_r - (I_{pL} + I_{jL} + I_{nL}) \\ &= I_{CT} + (I_{dL} + I'_{pL}) \\ &= I_{CT} + I_{VT} \end{aligned}$$

Here, there is a negligible change in the off-state electron tunnelling current due to the accumulation of holes at the surface.[5] Hence, the increase in device current due to optical excitation is $(I_{dL} + I'_{pL})$.

(ii) the junction hole diffusion current is of the same order of magnitude as either the junction recombination current or the light generated current components I_{dL} and I'_{pL}. This will occur for junction voltages of approximately greater than 0·3 V. In this case, hole injection from the p^+-substrate to the oxide-silicon interface takes place whereby the surface free-hole density will now consist of both photoholes and substrate holes. Assuming a negligible increase in the off-state electron tunnelling current,[5] the increase in the device current due to optical excitation will be the sum of I_{dL}, I'_{pL} and $I_{diff\,p}$.†

That is:

$$\begin{aligned} I_{AC_L} &= I_{diff\,p} + I_r - (I_{pL} + I_{jL} + I_{nL}) \\ &= I_{CT} + (I_{dL} + I'_{pL}) + I_{diff\,p} \\ &= I_{CT} + I_{VT} \end{aligned}$$

The optically generated current components can be seen to fit in well with the general concept of continuity of current flow throughout the device. It now remains to show experimentally the existence of these light current components.

6 Experimental results

A number of experimental devices have been fabricated on silicon wafers with a 20·6 μm epitaxial n-layer of 34 Ω cm resistivity, grown on a p^+-substrate of 0·01 Ω cm resistivity. The wafers were cleaned in a solution based on hydrogen peroxide.[9] This gave an oxide thickness of 13 Å before furnacing. The thin oxide was grown at 800° C for 5·5 min in dry oxygen and was then nitrogen annealed at the same temperature for 15 min. A final oxide thickness of 29 Å, as measured with an ellipsometer, was obtained. Aluminium contacts were deposited on the m.i.s.t. in a vacuum system of pressure less than 10^{-6} torr. The thin oxide cathode area was 40 μm x 40 μm while the p^+-n junction area was 1·4 mm x 1·4 mm.

In order to verify the existence of the light-generated current components, the following experimental measurements were taken:

(*a*) The increase in the m.i.s.t. off-state current at a fixed anode-cathode voltage was measured for various intensities of light. By ensuring that the p^+-n junction bias does not exceed 0·3 V, then these increases will be equal to the sum of I_{dL} and I'_{pL}, as discussed in Section 5.

(*b*) The photovoltaic increase in the junction voltage at zero anode-cathode bias was measured for various intensities of light. This increase should then be equal to the junction voltage required to produce the three photo currents $I_{pL}|_{W_{d=0}}$, I_{jL} and I_{nL}.

All measurements were taken using a Tektronix type 525 curve tracer. For ease of experimentation, a He-Ne red laser (optical wavelength $\lambda = 0{\cdot}6328\,\mu m$ and absorption depth $\alpha^{-1} = 2{\cdot}5\,\mu m$[6] was used. Furthermore, an optical test bench was set up in order to concentrate the incident optical power onto the most sensitive area of the m.i.s.t., which was found to be the thick oxide just outside the metal cathode. Here, the illuminated area was of the order of 5 μm x 5 μm.

Shown in Fig. 6 is a comparison of the experimentally measured increase in the off-state current of the m.i.s.t. biased at $V_{AC} = 5$ V, with the theoretical increase predicted by the sum of I_{dL} and I'_{pL} for three values of the device quantum efficiency η.[10, 11] Here the incident optical power was concentrated onto the thick oxide just off the metal cathode. During the course of the measurements the p^+-n junction voltage was not allowed to exceed 0·3 V. Under no incident optical power, the depth W_d of the surface depletion region at $V_{AC} = 5$ V was calculated to be 6·15 μm.[8] Under illumination W_d decreased at a rate of approximately 0·017 μm/μW. (See Appendix 11). Finally, as the device off-state current in the dark is recombination dominated ($I_{AC_d} = I_r = I_{CT}$), a value for the minority carrier hole diffusion length L_P may be calculated. This gave $L_p = 6\,\mu m$. In estimating L_p, the following points

† Recombination of injected holes in the neutral n-region must be taken into account when calculating $I_{diff\,p}$.

were taken into account:

(i) $L_p < W_d + W_n$

(ii) the p^+-n junction recombination and hole diffusion currents are strongly dependent on L_p, and are of the same order of magnitude at a junction voltage of approximately 0·4 − 0·5 V.[8]

The theoretical and experimental curves illustrated in Fig. 6 exhibit an approximately linear dependence on the incident optical power. This is sufficient to indicate that for junction voltages less than 0·3 V, the increase in the m.i.s.t. off-state current is due to the optical current components I_{dL} and I'_{pL}. The best fit between experiment and theory occurs for a quantum efficiency of approximately 0·85. It remains to be shown experimentally that as P, and hence the junction voltage, is increased, a third current component, namely I_{diffp}, becomes a major contributor to the increase in the device off-state current. Furthermore, it should be pointed out that if the diffusion photocurrent I'_{PL} is of the same order or greater than the drift photocurrent I_{dL}, then lateral diffusion effects must be considered. In our measurements however, the width of the surface depletion region is much greater than the absorption depth of the incident radiation. Hence I_{dL} is much greater than I'_{PL} so that lateral diffusion effects are minimised to such an extent as to be considered negligible.

If the incident radiation is concentrated just outside the cathode of the m.i.s.t. for the case of zero surface depletion region, then lateral diffusion effects will become dominant. To offset this, the device was uniformly illuminated whereby the illuminated area is equal to the junction cross-sectional area. The photocurrents $I_{pL}|_{W_{d=0}}$, I_{jL} and I_{nL} will flow in the m.i.s.t. which cause a photovoltaic voltage to appear across the otherwise zero biased p^+-n junction. The resulting junction current flows in opposition to the three photocurrents so that the external device current is zero. For junction voltages less than 0·3 V the junction current is recombination dominated. That is:[8]

$$I_r = \frac{qn_iW_jA_jD_p}{2L_p^2}\,(e^{qV_{AG}/2kT} - 1)$$

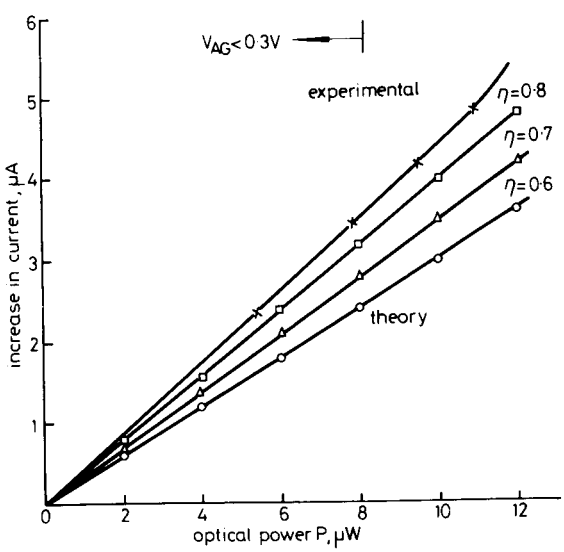

Fig. 6 *Experimental and theoretical increases in m.i.s.t. current I_{AC} at $V_{AC} = 5$ V and $V_{AG} < 0·3$ V, for different intensities of He-Ne light*

Lower three lines indicate theoretical predictions

$$= I_{pL}|_{W_{d=0}} + I_{jL} + I_{nL}$$

or

$$V_{AG} = \frac{2kT}{q} \ln\left[\frac{2L_p^2(I_{pL}|_{W_{d=0}} + I_{jL} + I_{nL})}{2n_iW_jA_jD_p} + 1\right] \quad (24)$$

where n_i is the intrinsic carrier concentration, A_j is the junction cross-sectional area and V_{AG} is the p^+-n junction or anode-to-gate voltage.

Illustrated in Fig. 7 is a comparison of the experimentally measured photovoltaic voltage of the m.i.s.t. on open circuit, with the theoretical increase predicted by eqn. 24 for three values of the device quantum efficiency η.[10, 11] Both the experimental and theoretical curves exhibit a logarithmic dependence on the incident optical power P. This is sufficient to indicate that the optical current components $I_{pL}|_{W_{d=0}}$, I_{jL} and I_{nL} are responsible for the observed photovoltaic effect. The discrepancies between the curves can be explained as being a result of uncertainty in the magnitude of the illuminated area‡ and the absolute value of the incident optical power P. The best fit between the experiment and theory occurs for a quantum efficiency of approximately 0·8 (cf. $\eta = 0·85$ for best fit in curves shown in Fig. 6).

7 Application as an optical threshold detector

Provided the sensitivity can be improved, and the switching speed is of the order of a few nanoseconds, the m.i.s.t. could be applied to optical communication systems as an optical threshold detector. Turn-on times of less than 2 ns, including delay, and turn-off times of less than 1 ns have been reported[13] on electrically switched devices. Similar optical switching speeds are envisaged, although for devices described in this paper, no attempt was made to optimise the fabrication process and geometry in order to produce high-speed devices.

At present, in high-speed fibre systems p-i-n or avalanche photodiodes are employed as photodetectors. However, as these diodes do not exhibit any switching property, extra circuitry is required to extract information from the received signal. The circuitry introduces unwanted noise which would not be present if an optical threshold detector were used. Thus, if the m.i.s.t. also proves to be no noiser

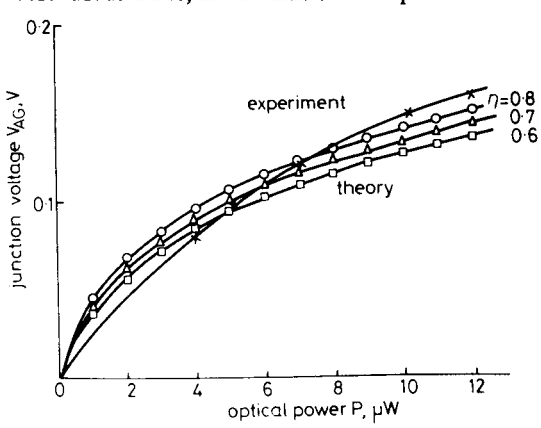

Fig. 7 *Experimental and theoretical increases in the junction voltage of the m.i.s.t. at $V_{AC} = 0$ V, for different intensities of He-Ne light*

‡ The devices tested were large-area devices and were not isolated during the fabrication process. Hence the junction cross-sectional area was not well defined.

than a *p-i-n* or avalanche photodiode, then a reduction in receiver noise as well as circuit complexity can be obtained with its use in optical transmission systems.

Finally, we note that as fibre systems incorporate optical sources operating in the 0·8–0·9 μm wavelength region, future experimental work on the m.i.s.t. as an optical switching device must be geared to this wavelength region.

8 Conclusion

In this paper we have considered the mechanism responsible for optically switching metal tunnel-insulator n-p^+ silicon devices. The 1-dimensional diffusion equation was employed to derive the light-generated minority carrier distributions and hence diffusion currents in the neutral n and p^+ regions, together with the photocurrents in the surface and junction depletion regions. For junction voltages less than approximately 0·3 V, the increase in the device off-state current is due to the optical current components I_{dL} and I'_{pL}, whereas for junction voltages above 0·3 V, a third current component, namely the junction hole diffusion current, becomes a major contributor to the increase in the device off-state current. Photocurrents I_{pL}, I_{jL} and I_{nL} were shown to contribute to a photovoltaic increase in the p^+-n junction voltage.

Experimental verification of the photocurrents and the photovoltaic effect was undertaken. The agreement obtained between the experimental and predicted results was sufficient to indicate that the optical current components derived in this paper exist and hence play an important role in the operation of the device.

Finally, the m.i.s.t. was shown to have potential as an optical threshold detector in high-speed optical-fibre systems provided certain levels of sensitivity, switching speed and noise performance are achieved.

9 Acknowledgments

The authors wish to thank the Radio Research Board of Australia for their financial support of the project.

10 References

1 SIMMONS, J.G., and EL-BADRY A.: 'Theory of switching phenomena in metal/semi-insulating/n-p^+ silicon devices', *Solid State Electron.*, 1977, **20**, pp. 955–961
2 EL-BADRY, A., and SIMMONS, J.G.: 'Experimental studies of switching in metal semi-insulating n-p^+ silicon devices', *ibid.*, 1977, 20, pp. 963–966
3 SIMMONS, J.G., and CHIK, D.K.: 'The metal-insulator-silicon thyristor' (to be published)
4 NASSIBIAN, A.G., CALLIGARO, R.B., and SIMMONS, J.G.: 'Digital optical metal insulator silicon thyristor (o.m.i.s.t.)', *IEE J. Solid-State & Electron. Devices*, 1978, 2, pp. 149–154
5 GREEN, M.A., and SHEWCHUN, J.: 'Current multiplication in metal-insulator-semiconductor (MIS) tunnel diodes', *Solid State Electron*, 1974, 17, pp. 349–365
6 SZE, S.M.: 'Physics of semiconductor devices' (Wiley, 1969)
7 WOLF, M.: 'Limitations and possibilities for improvement of photovoltaic solar energy converters. Pt. I: Consideration for earth's surface operation'., *Proc. IRE*, 1960, **48**, pp. 1246–1263
8 GROVE, A.S.: 'Physics and technology of semiconductor devices' (Wiley, 1967)
9 KERN, W, and PUOTINEN, D.A.: 'Cleaning solutions based on hydrogen peroxide for use in silicon semiconductor technology', *RCA Rev.* 1970, **31**, pp. 187–206
10 BRUGLER, J.S.: 'Optoelectronic nomenclature for solid-state radiation detectors and emitters', *IEEE J. Solid-State Circuits*, 1970, SC-5, pp. 276–283
11 SCHNEIDER, M.V.: 'Schotty barrier photodiodes with anti-reflection coating', *Bell. Syst. Tech. J.*, 1967, **45**, pp. 1611–1638
12 NASSIBIAN, A.G., and CALLIGARO, R.B.: 'Surface state charge in thin oxide m.i.s.t. devices', *IEE J. Solid-State & Electron. Devices*, 1979, 3, pp. 6–10
13 YAMAMOTO, T., KAWAMURA, K., and SHIMIZU, H.: 'Silicon p-N insulator-metal (p-N-I-M) devices', *Solid-State Electron*, 1976, 19, pp. 701–706

11 Appendix

The width W_d of the surface depletion region is given by:[8]

$$W_d = \left(\frac{2\epsilon_s \psi_s}{qN_D}\right)^{1/2} \tag{25}$$

where ϵ_s is the semiconductor permittivity, N_D is the density of electrons in the neutral n-layer, and ψ_s is the surface potential.

The surface potential can be calculated by considering the total voltage across the device. That is, with the m.i.s.t. not illuminated, we have

$$V_{AC_d} = \psi_{s_d} + V_{ox_d} + V_{AG_d} + V_{FB} \tag{26}$$

where V_{AC}, V_{ox}, V_{AG} and V_{FB} refer to the anode-cathode voltage, oxide voltage, anode-gate (p^+-n junction) voltage and flat-band voltage, respectively. The subscript d indicates that measurements are taken in the dark.

The oxide voltage in the dark can be written as:[8]

$$V_{ox_d} = \frac{Q_s}{C_{ox}} = \frac{qN_D W_d}{C_{ox}} = \frac{(2qN_D\epsilon_s\psi_{s_d})^{1/2} d_{ox}}{\epsilon_{ox}}$$

$$\simeq 0{\cdot}0082\,(\psi_{s_d})^{1/2}$$

where the surface space charge per unit area is

$$Q_s = qN_D W_d = (2qN_D\epsilon_s\psi_{s_d})^{1/2}\ \mathrm{C/m^2}$$

and the oxide capacitance is:

$$C_{ox} = \frac{\epsilon_{ox}}{d_{ox}}\ \mathrm{F/m^2}$$

Neglecting the oxide voltage, eqn. 26 may be rewritten as

$$\psi_{s_d} = V_{AC_d} - V_{FB} - V_{AG_d}$$

where V_{AC_d} is kept constant at 5 V, and V_{AG_d} is measured experimentally. The flatband voltage for this particular device was approximately 0·5 V.[12] Hence ψ_{s_d} and W_d may be calculated, giving $\psi_{s_d} \simeq 4{\cdot}38$ V and $W_d = 4{\cdot}35\,\mu$m.

Keeping the anode-cathode voltage constant while illuminating the m.i.s.t., the p^+-n junction voltage increases, thus decreasing both the surface potential and the surface depletion region width. Ignoring the oxide voltage, the off-state surface potential under illumination becomes

$$\psi_{s_L} = V_{AC_d} - V_{FB} - V_{AG_L}$$

where

$$V_{AG_L} > V_{AG_d}$$

or

$$\psi_{s_L} = \psi_{s_d} + V_{AG_d} - V_{AG_L}$$

The corresponding depletion width is then obtained from eqn. 25. It was found experimentally that W_d decreased at a rate of approximately 0·017 μm/μW.